Chemical Science

ROYAL SOCIETY OF CHEMISTRY

EDGE ARTICLE

View Article Online
View Journal | View Issue

Cite this: *Chem. Sci.*, 2022, **13**, 1693

All publication charges for this article have been paid for by the Royal Society of Chemistry

Received 24th November 2021
Accepted 16th January 2022

DOI: 10.1039/d1sc06563g

rsc.li/chemical-science

Cu(II)-based DNA labeling identifies the structural link between transcriptional activation and termination in a metalloregulator†

Joshua Casto, [a] Alysia Mandato,[a] Lukas Hofmann,[b] Idan Yakobov,[b] Shreya Ghosh, [a] Sharon Ruthstein *[b] and Sunil Saxena *[a]

Understanding the structural and mechanistic details of protein-DNA interactions that lead to cellular defence against toxic metal ions in pathogenic bacteria can lead to new ways of combating their virulence. Herein, we examine the Copper Efflux Regulator (CueR) protein, a transcription factor which interacts with DNA to generate proteins that ameliorate excess free Cu(I). We exploit site directed Cu(II) labeling to measure the conformational changes in DNA as a function of protein and Cu(I) concentration. Unexpectedly, the EPR data indicate that the protein can bend the DNA at high protein concentrations *even* in the Cu(I)-free state. On the other hand, the bent state of the DNA is accessed at a low protein concentration in the presence of Cu(I). Such bending enables the coordination of the DNA with RNA polymerase. Taken together, the results lead to a structural understanding of how transcription is activated in response to Cu(I) stress and how Cu(I)-free CueR can replace Cu(I)-bound CueR in the protein-DNA complex to terminate transcription. This work also highlights the utility of EPR to measure structural data under conditions that are difficult to access in order to shed light on protein function.

Introduction

Metalloregulator proteins are transcription factors that perform a crucial role in the cellular defense of pathogenic bacteria by maintaining metal homeostasis.[1] For example, while copper ions are essential for several important enzymes due to favorable redox properties, excess free copper ions induce cytotoxicity by participating in Fenton and Haber–Weiss-like reactions that produce biologically lethal hydroxyl radicals and carbonate ions.[2,3] Cells have, therefore, evolved elaborate protective mechanisms to eliminate excess free copper. The copper efflux metalloregulator (CueR) in *E. coli* binds Cu(I) in the cell with an affinity of 10^{21} M and specific DNA sequences to activate the transcription of cueO or copA genes.[4] The protein cueO oxidizes Cu(I) to less cytotoxic Cu(II), whereas copA is a transmembrane pump that exports free Cu(I) out of the cytosol. Single molecule fluorescence resonance energy transfer (smFRET) measurements[4] indicate that the CueR transcription regulation mechanism can be thought of as a cycle depicted in Fig. 1.

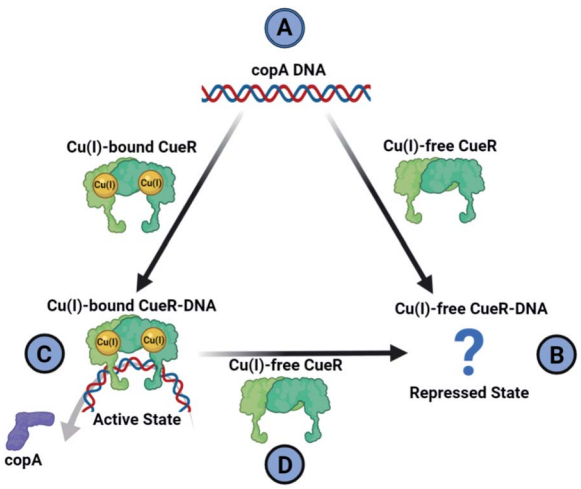

Term	Description
apo-CueR	*Cu(I)-free CueR*
holo-CueR	*Cu(I)-bound CueR*
Repressed state	*apo-CueR bound to DNA*
Active State	*holo-CueR bound to DNA*

Fig. 1 Cartoon representation of the CueR transcription regulation mechanism. (A) DNA containing copA sequence (B) Cu(I)-free CueR binds to DNA to form a repressed complex but there is limited structural data in this state. (C) CueR bound with Cu(I) kinks DNA and promotes RNAp coordination to the complex to begin the transcription of copA. (D) To terminate transcription, Cu(I)-free CueR replaces Cu(I)-bound CueR in the protein-DNA complex. A glossary of alternative terminology for CueR functional states is provided below the cycle cartoon.

[a]*Department of Chemistry, University of Pittsburgh, Pittsburgh, Pennsylvania 15260, USA. E-mail: sksaxena@pitt.edu*

[b]*Department of Chemistry, Faculty of Exact Sciences, The Institution of Nanotechnology and Advanced Materials, Bar-Ilan University, Ramat-Gan 5290002, Israel. E-mail: Sharon.Ruthstein@biu.ac.il*

† Electronic supplementary information (ESI) available. See DOI: 10.1039/d1sc06563g

In this mechanism, the binding of Cu(I)-free CueR (*i.e.* apo CueR) to DNA putatively leads to a repressed state wherein transcription cannot occur (Fig. 1B). On the other hand, the binding of Cu(I)-bound CueR is critical to promoting the interaction with RNA polymerase (RNAp) to initiate transcription (Fig. 1C).[5] Once Cu(I) concentrations fall below cytotoxic thresholds in the cell, transcription needs to be deactivated. Due to the 10^{21} M affinity[4] of CueR to Cu(I), termination *via* dissociation of Cu(I) from CueR is unlikely. Alternatively, smFRET results suggest a substitution mechanism where Cu(I)-free CueR replaces Cu(I)-bound CueR on the DNA to end transcription (Fig. 1D).[6]

Crucially, therefore, the competition between Cu(I)-free CueR *vs.* Cu(I)-bound CueR for DNA is key to both activation and termination of transcription (Fig. 1C and D). However, despite much work there is still a lack of structural evidence that depicts how Cu(I)-free CueR participates in both repression and termination. Crystal[7] and cryo-EM structures[8,9] both show that Cu(I)-bound CueR bends the DNA. Alternatively, the crystal structure of the Cu(I)-free CueR–DNA complex[7] indicates that the DNA is undistorted. These data pose an intriguing conundrum. How does Cu(I)-free CueR replace Cu(I)-bound CueR on a kinked duplex if it only coordinates to an undistorted duplex (Fig. 1B and D)?

Results and discussion

Herein we use pulsed Electron Paramagnetic Resonance (EPR) techniques to directly measure the conformational changes of the DNA at key steps of the regulation mechanism to elucidate the structural relationship between transcription activation, repression, and termination.

Fig. 2A shows the DNA used for EPR measurements. The protein-binding sites of the copA DNA sequence are highlighted in grey. Each DNA strand contains a 2,2-dipicolylamine (DPA) phosphoramidite moiety that chelates Cu(II). The DPA residues, therefore, allow for attachment of two Cu(II) labels separated by 12 base pairs. The DPA-Cu(II) motif is a straightforward spin labeling technique that orients the DPA into the helix and reports directly on DNA backbone distances.[10,11] Additionally, we have shown earlier that orientational selectivity[12,13] effects for the DPA-Cu(II) motif are negligible even at Q-band, which enables the measurement of distances even from data at a single magnetic field.[11] The labeling of DNA with Cu(II) is described in ESI.†[11,14] Electrophoretic mobility shift assays (EMSA) show that CueR binds to the DPA-DNA duplex (Fig. S1†). Note that the native metal binding site in CueR coordinates only monovalent ions.[15]

All EPR data were acquired in *N*-ethylmorpholine (NEM) buffer in order to ensure that free Cu(II) was EPR silent.[16,17] Continuous wave (CW)-EPR experiments were performed to characterize sample Cu(II) coordination (*cf.* ESI Fig. S2†). Each CW spectrum consisted of a dominant component with hyperfine splitting characteristic of DPA-Cu(II) coordination.[18] UV/vis measurements show no reduction of excess Cu(II) to Cu(I) (*cf.* Fig. S3†). Additional details of the sample preparation and experimental parameters are described further in the ESI.†

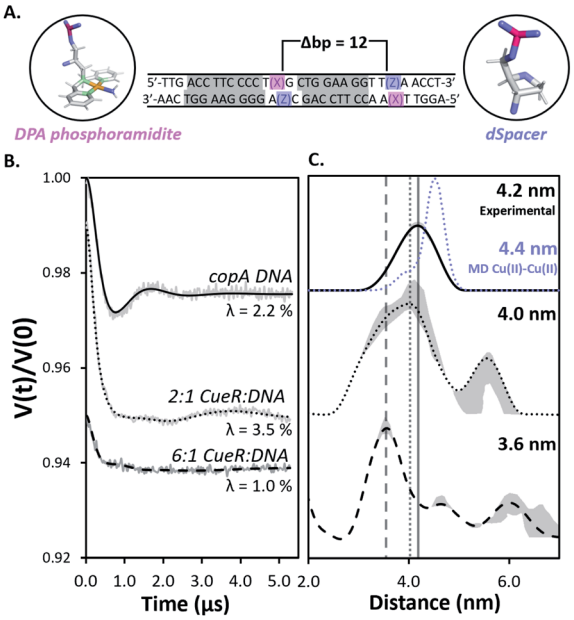

Fig. 2 (A) The 31 bp copA DNA sequence. DPA (pink) and dSpacer (blue) moieties were substituted into nucleotide positions that do not interact with CueR. The Cu(II) coordinates to DPA leading to two Cu(II) positioned 12 bp apart. The protein binding sites are highlighted in grey. (B) Background subtracted DEER time traces for the copA DNA and the duplex bound to CueR at different concentration ratios of protein to duplex. Modulation depths (λ) are shown. (C) The validated Cu(II)–Cu(II) distance distributions in copA DNA, 2 : 1 CueR : DNA, and 6 : 1 CueR : DNA samples. The analysis was performed using DeerAnalysis. The Cu(II)–Cu(II) distance distribution from MD for copA DNA is presented as the blue dots. The MD and EPR distance distributions for copA DNA are normalized with respect to their probabilities. Upon increasing the ratio of protein to duplex from 2 : 1 to 6 : 1, the most probable distance decreases from 4.2 nm to 3.6 nm. The grey lines represent the most probable distance of each sample to provide a visual aid for comparison. The grey regions show the validated distribution from DEERAnalysis (details are provided in the ESI†). ComparativeDEERAnalysis consensus distance distributions are provided in the ESI (Fig. S7†).

Next, double electron electron resonance[19,20] (DEER) was performed to measure the distance distribution between the two Cu(II)–Cu(II) sites (*cf.* Fig. 1A). The primary DEER traces, basis EPR data, and biological repeats for all samples are provided in ESI (Fig. S4 and S5†). DEER data with optimal dipolar evolution times were achieved by using deuterated solvents and glycerol to increase the relaxation times of Cu(II) spin labels[21] (Fig. S6†). First, DEER was performed on free DNA and then on the 2 : 1 CueR : DNA sample (Fig. 2B). The resulting distance distribution obtained from the background subtracted DEER time trace of the free duplex analyzed with DEERAnalysis[22] returns a most probable distance centered at 4.2 nm (Fig. 2B). Such a distance is anticipated for a 12 base pair separation of a typical B-DNA and agrees well with a 2.25 μs molecular dynamics (MD) simulation of five averaged 450 ns replicates.

The DEER time trace of the 2 : 1 protein to DNA sample is distinctly different compared to the free DNA, which clearly

indicates a different conformational ensemble for the DNA. An analysis of the distance distribution by DeerAnalysis reveals a bimodal distribution (Fig. 2C center panel). ComparativeDEERAnalysis consensus distance distributions utilizing DEERNet[23] and automated Tikhonov regularization fitting show similar bimodal distributions as well (Fig. S7†). We attribute the larger distance at 5.7 nm to high order binding, where CueR oligomers and multiple DNA come together. Such high order binding is commonly seen in nucleoprotein complexes that require thermodynamically unfavorable distortion of the DNA.[24,25] Therefore, two different DNA strands in the higher order nucleoprotein complex would give rise to a range of distances outside what is feasible for a 12 bp separation. When comparing the DEER traces from copA DNA and 2 : 1 CueR–DNA time traces, the modulation depth increases from 2.2% to 3.5% (Fig. 2A). This increase in modulation depth is consistent with the presence of higher order complexes.[26–28] Additionally, the EMSA data corroborates the presence of species with quadruplexes (Fig. S1†). In subsequent discussion, we focus on the more biophysically relevant distribution centered around 4.2 nm.

The distribution corresponding to the *ca.* 4.2 nm distance appears to broaden in the presence of a two-fold excess of CueR (Fig. 2C, top *vs.* middle panel). We hypothesize that this broadening may be due to the presence of bent and undistorted DNA in solution. The presence of the undistorted DNA is either from free DNA or from CueR–DNA complex with undistorted DNA. To test this hypothesis, we measured the DEER signal for a 6 : 1 ratio of protein to DNA. In this case a peak at 3.6 nm becomes dominant. The shortening of the distance is likely due to the DNA kinking upon protein binding. Prior work has shown that the Cu(II)–Cu(II) distance in DNA can be directly related to the backbone C′–C′ distance.[14] A more careful model analysis that accounts for the positioning of the Cu(II) atoms with respect to the DNA backbone, yields a 5′ end – center – 3′ end angle of 55° for the duplex with a 3.6 nm Cu(II)–Cu(II) distance (Fig. S8†). Such a bending of the duplex makes sense as this DNA sequence has a 19 bp separation between the regions which interact with RNAp. Bending of the DNA brings sites needed for RNAp coordination on the same face of the DNA, which promotes transcription.[9,29,30]

The data with a CueR : DNA ratio of 6 : 1 supports the hypothesis that at a ratio of at least 2 : 1 there is coexistence of undistorted DNA and a kinked DNA complex. However, as more CueR is added into the system, the kinked DNA complex becomes dominant. This concentration dependence is anticipated due to a lower affinity of Cu(I)-free CueR to DNA.[5]

The formation of a kinked duplex in the presence of Cu(I)-free CueR is in apparent contradiction to the available crystal structure of the Cu(I)-free CueR–DNA complex (PDB: 4WLS) which shows an undistorted DNA (*cf.* Fig. S9† for details).[7] More importantly, the crystal structure was solved using an approximate concentration ratio of 1 : 2 CueR dimer to DNA. This observation is unsurprising based on the DEER data, since even at 2 : 1 protein to DNA ratio the dominant conformation corresponds to the undistorted DNA. More importantly, a key insight from our solution data is that higher concentrations of CueR promotes the formation of the kinked DNA complex, even in the absence of Cu(I). The observation that Cu(I)-free CueR can induce duplex kinking provides a clear structural understanding for how Cu(I)-free CueR can substitute and remove Cu(I)-bound CueR on kinked DNA to end transcription (see below).

Next, we examined the DNA structure in the Cu(I)-bound CueR–DNA complexes. Given that recent results have suggested that there are more than two Cu(I) binding sites in CueR,[31] we measured DEER time traces for 2 : 1 and 6 : 1 dimer to duplex at three different Cu(I) equivalents (Fig. 3). Notably the time traces for all six samples in Fig. 3A are similar, suggesting some uniformity among the spin pair ensembles. Importantly, the presence of Cu(I) promotes the formation of a 3.7 nm distance (within experimental error of the previously observed 3.6 nm) *readily* even at a 2 : 1 ratio of protein to DNA (*cf.* compare Fig. 3B to Fig. 2C). Negligible differences in the distances are observed as Cu(I) concentrations are increased in both the 2 : 1 and 6 : 1 complexes as anticipated from the time traces in Fig. 3A. The presence of a kinked DNA in the Cu(I)-bound CueR–DNA complex is consistent with the crystal structure of the complex measured using Ag(I) as a surrogate

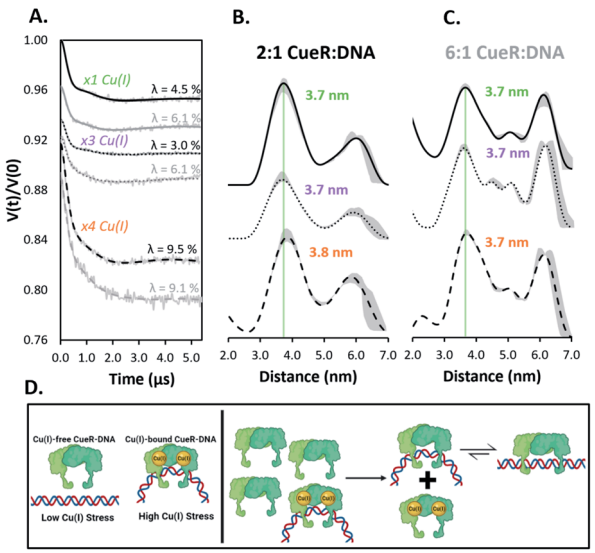

Fig. 3 (A) Background subtracted DEER time traces for the copA DNA at varying CueR dimer to duplex ratios (2 : 1 black, 6 : 1 grey) and monomeric equivalents of Cu(I). Modulation depths (λ) are shown. (B and C) Distance distributions of CueR complex ratios with equivalents of Cu(I) per dimer as described. Distributions were obtained from their respective time traces using DeerAnalysis. ComparativeDEERAnalysis consensus distance distributions are provided in the ESI (Fig. S7†). The green dashed line is a visual aid to compare the most probable distances. The grey regions show the validated distribution from DEERAnalysis (details are provided in the ESI†). (D) Pictorial summary of the presented work. Under high Cu(I) stress, the Cu(I)-bound CueR–DNA complex with a bent DNA is formed to promote transcription. After Cu(I) homeostasis is restored, a surge of Cu(I)-free CueR can readily substitute Cu(I)-bound CueR on DNA to end transcription, since Cu(I)-free CueR can bind in the bent state. Subsequently, Cu(I)-free CueR can interconvert to a thermodynamically favorable linear duplex state or unbind, in order to end transcription.

for Cu(I) (PDB: 4WLW).[7] A detailed analysis is provided in the ESI (Fig. S9†).

Additionally, modulation depths of *ca.* 9% were observed with ×4 equivalents of Cu(I) per CueR monomer (Fig. 3A). A consistent increase of modulation depth for these samples further supports the claim that additional spin pairs form *via* high order binding. The greater modulation depths for the Cu(I)-bound CueR–DNA complexes compared to the Cu(I)-free protein complexes suggest a greater amount of high order binding occurring in the presence of Cu(I).

Importantly, the data suggest that the presence of Cu(I) plays a key role in DNA distortion. A distorted DNA is observed even at a lower ratio of protein to DNA compared to the Cu(I)-free CueR–DNA case (*cf.* Fig. 2). Thus, Cu(I) acts as the key to drive the dominant formation of the kinked DNA complex that will allow RNAp coordination for transcription (Fig. 1C and D).

Conclusions

In summary, these EPR results, used in conjunction with insight gained from prior biochemical,[4] smFRET,[6] and structural measurements,[7] provide a deeper understanding of transcription activation and termination in *E. coli*. We have shown that Cu(I)-free CueR can distort DNA in a similar fashion as Cu(I)-bound CueR (*cf.* Fig. 2 *vs.* Fig. 3), but a large concentration of Cu(I)-free CueR is needed to bend the DNA. Under normal conditions a large concentration of CueR is unlikely in *E. coli* cells, given that CueR is expressed through copper sensing mechanisms that activate in response to the presence of Cu(I).[32,33] Thus, the copA expression is not activated (*cf.* Fig. 3D, left panel). On the other hand, the presence of even a small amount of Cu(I) generates a Cu(I)-bound CueR–DNA complex in which the DNA is bent, leading to the activation of transcription and the remediation response (Fig. 3D, left panel). When Cu(I) homeostasis is restored, there now exists an excess of Cu(I)-free CueR created by copper sensing. The substitution of Cu(I)-bound CueR by a single Cu(I)-free CueR becomes thermodynamically and kinetically straightforward as minimal structural perturbation of DNA is needed (Fig. 3D, right panel). This complex can then transition to a state with an undistorted DNA or the Cu(I)-free CueR can dissociate from the duplex to end transcription. Indeed, the presence of a Cu(I)-free CueR-undistorted DNA complex and unbinding has been inferred from smFRET results.[6] These data, taken together with recent results using Cu(II) labeling of the CueR,[34] illustrate the potential of site-directed Cu(II) labeling. More broadly, this work highlights the utility of such DNA labeling approaches[35–37] to enable the measurement of conformational ensembles under conditions that are not easily accessible (*e.g.* concentration dependent measurements in this case) in order to generate a more holistic picture of protein function. In the future, incorporating RNAp into our measurements would allow for a direct comparison to cryo-EM structures[8,9] and permit the capturing of structural details for the DNA transcription bubble in solution.

Data availability

The data supporting this work have been uploaded as part of the ESI:†

Protein purification and expression, sample preparations, EMSA assay methods, MD simulation details, CW-EPR spectra and simulations, raw DEER data, biological replicate DEER data, primary DEER data, comparative method analysis for DEER time trace fitting, DNA bending model, EPR and crystal structure data comparisons.

Raw and processed datasets are available for preview and download at DOI: 10.17632/zrxjrc7fgn.1.

Author contributions

J. C. expressed, purified, and prepared the protein used with DNA samples. J. C. also carried out the primary investigation and analysis of EPR data. A. M. conducted the MD simulations and created the bent duplex model. L. H. and I. Y. provided initial protein resources, EMSA data, the protein plasmid used for expression, and aided with project development. S. G. was responsible for initial project development. S. R. and S. S. supervised all aspects of the research. J. C., S. R., and S. S. wrote the manuscript. All authors reviewed the manuscript.

Conflicts of interest

The authors declare no competing financial interests.

Acknowledgements

We thank Riti Sen and Dr Xing Yee Gan at the University of Pittsburgh for their time and assistance with respect to preparation and storage of air sensitive stock solutions used in this work. We also thank Dr Lada Gevorkyan-Airapetov for her assistance with the EMSA experiments. All MD simulations were carried out at the University of Pittsburgh Center for Research Computing. Cartoon figures were created with http://Biorender.com. S. S. and S. R. acknowledge the support from the National Science Foundation-Binational Science Foundation (NSF-BSF, NSF no. MCB-2006154; BSF. 2019723).

References

1 D. P. Giedroc and A. I. Arunkumar, *Dalton Trans.*, 2007, **29**, 3107–3120.
2 J. M. Argüello, D. Raimunda and T. Padilla-Benavides, *Front. Cell. Infect. Microbiol.*, 2013, **3**, 1–14.
3 A. M. Fleming and C. J. Burrows, *Chem. Soc. Rev.*, 2020, **49**, 6524–6528.
4 F. W. Outten, C. E. Outten, J. Hale and T. V. O'Halloran, *J. Biol. Chem.*, 2000, **275**(40), 31024–31029.
5 D. J. Martell, C. P. Joshi, A. Gaballa, A. G. Santiago, T. Y. Chen, W. Jung, J. D. Helmann and P. Chen, *PNAS*, 2015, **112**(44), 13467–13472.

6 C. P. Joshi, D. Panda, D. J. Martell, N. M. Andoy, T.-Y. Chen, A. Gaballa, J. D. Helmann and P. Chen, *PNAS*, 2012, **109**(38), 15121–15126.
7 S. J. Philips, M. Canalizo-Hernandez, I. Yildirim, G. C. Schatz, A. Mondragón and T. V. O'Halloran, *Science*, 2015, **349**(6250), 877–881.
8 C. Fang, S. J. Philips, X. Wu, K. Chen, J. Shi, L. Shen, J. Xu, Y. Feng, T. V. O'Halloran and Y. Zhang, *Nat. Chem. Biol.*, 2021, **17**, 57–64.
9 W. Shi, B. Zhang, Y. Jiang, C. Liu, W. Zhou, M. Chen, Y. Yang, Y. Hu and B. Liu, *iScience*, 2021, **24**(5), 102449.
10 M. J. Lawless, J. L. Sarver and S. Saxena, *Angew. Chem., Int. Ed.*, 2017, **56**(8), 2115–2117.
11 A. Gamble Jarvi, X. Bogetti, K. Singewald, S. Ghosh and S. Saxena, *Acc. Chem. Res.*, 2021, **54**(6), 1481–1491.
12 Z. Yang, M. Ji and S. Saxena, *Appl. Magn. Reson.*, 2010, **39**, 487–500.
13 J. E. Lovett, A. M. Bowen, C. R. T. Timmel, M. W. Jones, J. R. Dilworth, D. Caprotti, S. G. Bell, L. L. Wong and J. Harmer, *Phys. Chem. Chem. Phys.*, 2009, **11**, 6840–6848.
14 S. Ghosh, J. Casto, X. Bogetti, C. Arora, J. Wang and S. Saxena, *Phys. Chem. Chem. Phys.*, 2020, **22**(46), 26707–26719.
15 A. Changela, K. Chen, Y. Xue, J. Holschen, C. E. Outten, T. V. O'Halloran and A. Mondragon, *Science*, 2003, **301**(5638), 1383–1387.
16 C. D. Syme, R. C. Nadal, S. E. J. Rigby and J. H. Viles, *J. Biol. Chem.*, 2004, **279**(18), 18169–18177.
17 B. K. Shin and S. Saxena, *J. Phys. Chem. A*, 2011, **115**(34), 9590–9602.
18 S. Ghosh, M. J. Lawless, H. J. Brubaker, K. Singewald, M. R. Kurpiewski, L. Jen-Jacobson and S. Saxena, *Nucleic Acids Res.*, 2020, **48**(9), 1–11.
19 A. D. Milov, A. G. Maryasov and Y. D. Tsvetkov, Pulsed Electron, *Appl. Magn. Reson.*, 1998, **15**, 107–143.
20 M. Pannier, S. Veit, A. Godt, G. Jeschke and H. W. Spiess, *J. Magn. Reson.*, 2000, **142**(2), 331–340.
21 J. Casto, A. Mandato and S. Saxena, *J. Phys. Chem. Lett.*, 2021, **12**(19), 4681–4685.
22 G. Jeschke, V. Chechik, P. Ionita, A. Godt, H. Zimmermann, J. Banham, C. R. Timmel, D. Hilger and H. Jung, *Appl. Magn. Reson.*, 2006, **30**, 473–498.
23 S. G. Worswick, J. A. Spencer, G. Jeschke and I. Kuprov, *Sci. Adv.*, 2018, **4**(8), 1–17.
24 W. Jung, K. Sengupta, B. M. Wendel, J. D. Helmann and P. Chen, *Nucleic Acids Res.*, 2020, **48**(5), 2199–2208.
25 R. Grosschedl, *Curr. Opin. Cell Biol.*, 1995, **7**(3), 362–370.
26 B. E. Bode, D. Margraf, J. Plackmeyer, D. Dürner, T. F. Prisner and O. Schiemann, *J. Am. Chem. Soc.*, 2007, **129**(21), 6736–6745.
27 A. Gamble Jarvi, A. Sargun, X. Bogetti, J. Wang, C. Achim and S. Saxena, *J. Phys. Chem. B*, 2020, **124**(35), 7544–7556.
28 M. J. Lawless, S. Ghosh, T. F. Cunningham, A. Shimshi and S. Saxena, *Phys. Chem. Chem. Phys.*, 2017, **19**(31), 20959–20967.
29 A. Z. Ansari, J. E. Bradner and T. V. O'Halloran, *Nat*, 1995, **374**, 370–375.
30 A. Z. Ansari, M. L. Chael and T. V. O'Halloran, *Nat*, 1992, **355**, 87–89.
31 R. K. Balogh, B. Gyurcsik, E. Hunyadi-Gulyas, J. Schell, P. W. Thulstrup, L. Hemmingsen and A. Jancso, *Chemistry*, 2019, **25**(66), 15030–15035.
32 K. Yamamoto and A. Ishihama, *Mol. Microbiol.*, 2005, **56**(1), 215–227.
33 K. S. Chaturvedi and J. P. Henderson, *Frontiers in Cellular and Infection Microbiology*, 2014, 1–12.
34 H. Sameach, S. Ghosh, L. Gevorkyan-Airapetov, S. Saxena and S. Ruthstein, *Angew. Chem., Int. Ed.*, 2019, **58**(10), 3053–3056.
35 C. M. Grytz, A. Marko, P. Cekan, S. T. Sigurdsson and T. F. Prisner, *Phys. Chem. Chem. Phys.*, 2016, **18**(4), 2993–3002.
36 G. W. Reginsson, S. A. Shelke, C. Rouillon, M. F. White, S. T. Sigurdsson and O. Schiemann, *Nucleic Acids Res.*, 2013, **41**(1), 1–10.
37 G. Y. Shevelev, O. A. Krumkacheva, A. A. Lomzov, A. A. Kuzhelev, O. Y. Rogozhnikova, D. V. Trukhin, T. I. Troitskaya, V. M. Tormyshev, M. V. Fedin and D. V. Pyshnyi, *J. Am. Chem. Soc.*, 2014, **136**(28), 9874–9877.